


The Application of Radiomics in Breast MRI: A Review

Technology in Cancer Research & Treatment
Volume 19: 1-16
© The Author(s) 2020
Article reuse guidelines:
sagepub.com/journals-permissions
DOI: 10.1177/1533033820916191
journals.sagepub.com/home/tct



Dong-Man Ye, MD¹ , Hao-Tian Wang, BS², and Tao Yu, PhD¹

Abstract

Breast cancer has been a worldwide burden of women's health. Although concerns have been raised for early diagnosis and timely treatment, the efforts are still needed for precision medicine and individualized treatment. Radiomics is a new technology with immense potential to obtain mineable data to provide rich information about the diagnosis and prognosis of breast cancer. In our study, we introduced the workflow and application of radiomics as well as its outlook and challenges based on published studies. Radiomics has the potential ability to differentiate between malignant and benign breast lesions, predict axillary lymph node status, molecular subtypes of breast cancer, tumor response to chemotherapy, and survival outcomes. Our study aimed to help clinicians and radiologists to know the basic information of radiomics and encourage cooperation with scientists to mine data for better application in clinical practice.

Keywords

breast cancer, radiomics, magnetic resonance imaging, MRI, application, prognosis

Abbreviations

ADC, apparent diffusion coefficient; ALND, axillary lymph node dissection; ALNM, axillary Lymph Node Metastasis; AUC, area under the curve; BPE, background parenchymal enhancement; CE2, second postcontrast phase; CT, computed tomography; DCE, dynamic contrast-enhanced; DTI, diffusion tensor imaging; DWI, diffusion-weighted imaging; ER+, positive estrogen receptor; GLCM, gray-level co-occurrence matrix; HER2, human epidermal growth factor receptor 2; IHC, immunohistochemical; IVIM, intravoxel incoherent motion; LN, lymph node; LNM, lymph node metastasis; MRI, magnetic resonance imaging; NAC, neoadjuvant chemotherapy; pCR, pathological complete response; PET, positron emission tomography; PR+, positive progesterone receptor; SER, signal enhancement ratio; SLNB, sentinel lymph node biopsy; TIWI, T1-weighted image; T2WI, T2-weighted image; TN, triple negative; US, ultrasound

Received: November 22, 2019; Revised: January 21, 2020; Accepted: February 27, 2020.

Introduction

Breast cancer has been a worldwide burden of women's health, with an increasing trend in incidence in recent decades.¹ As the concerns of breast cancer have been raised to improve primary and secondary prevention, 5-year survival of breast cancer has increased steadily in most developed countries.² However, the efforts for early diagnosis and timely treatment are still warranted to reduce mortality. The concept of Breast Imaging Reporting and Data System has been proposed and widely used for more clear and uniform communication of clinicians and radiologists based on radiographic features to evaluate the classification and gradation of tumors. This classification remains limitations, as it greatly depends on the experience of radiologists. Patients with a suspected breast lesion are suggested to take a biopsy to confirm the

tumor nature before the surgery. Although biopsy can provide gold standard of suspicious breast lesions, it still has some limitations. As it is invasive and could not reflect the

¹ Department of Medical Imaging, Cancer Hospital of China Medical University, Liaoning Cancer Hospital & Institute, Shenyang, Liaoning Province, People's Republic of China

² Dalian Medical University, The First Clinical College, Dalian, Liaoning Province, People's Republic of China

Corresponding Author:

Tao Yu, Department of Medical Imaging, Cancer Hospital of China Medical University, Liaoning Cancer Hospital & Institute, No.44 Xiaoheyuan Road, Dadong District, Shenyang, Liaoning Province 110042, People's Republic of China.

Email: yutao@cancerhosp-ln-cmu.com



heterogeneity of the whole tumor that may provide uncertain information of lesions if the tumor size is too large.

Image technologies are the most direct and convenient tools to reflect the size, morphology, and radiographic characteristics of tumors that can be utilized to diagnosis, treatment, prognosis assessment, and so on. New technologies based on different imaging modalities have emerged for precision medicine and individualized treatment of patients with cancer. Since 2012, the concept of “radiomics” was firstly proposed by a Dutch researcher and interpreted as “the extraction of numerous features from radiographic imaging by a high-throughput approach.”³ Radiomics is a noninvasive imaging technology and has immense potential to obtain mineable data and evaluate whole tumor features of imaging.^{4,5} The information hidden from the assessment of human eyes can be used to build predictive models of clinical outcomes and provide a noninvasive and complementary method for tumor genotype. Radiomics has shown promise to be an imaging biomarker of different tumors in clinical practice.

Ultrasound (US), mammography, and magnetic resonance imaging (MRI) are the most common tools for breast examination in clinical practice. In our study, we only focused on the role of MRI in the application of radiomics. The Pubmed, Web of Science, and Embase were searched up to April 2019 by using search strategies. We used Mesh terms (Medical subject heading) “breast cancer” and “magnetic resonance imaging” and “radiomics” or “texture analyses” or “quantitative analyses,” as well as adding free words in different combination for avoiding the omission of the related literatures. In this study, we aimed to provide a comprehensive review which focused on basic information and the application of radiomics for oncologists. In addition, we concluded the major characteristics, such as study design, the number of patients, MRI modality, magnetic field, radiomics features, and outcomes to provide information of the studies which evaluated various clinical applications (Tables 1-5).

The Workflow of Radiomics

Images from US, computed tomography (CT), MRI, and positron emission tomography (PET) have been widely used for radiomics analysis in scientific fields. Ultrasound and CT provide structural features of tumors, while PET and MRI provide functional and molecular information. Computed tomography was firstly applied in radiomics and then MRI was the second, and these technologies were also the most common modalities in radiomics.^{3,4} As the Quantitative Imaging Network guidelines were established by the National Cancer Institute in 2012, the workflow of radiomics included: (1) image acquisition and reconstruction, (2) lesion segmentation, (3) feature extraction, and (4) data analysis.⁵³

The first step of radiomics analysis is the assessment of high quality and normalized images. Most data of published studies were retrospectively extracted from hospital-based imaging database. It is worth noting that images with different modalities, protocols, and reconstructions from various hospital databases

may contribute to some differences in radiomics models.⁵⁴ Then the delineation of the lesion is conducted based on standard-of-care images. The whole tumor is segmented by manual, semi-manual, and automatic methods.⁵³ The process of segmentation should be accurate, reproducible, and reliable. Manual segmentation by experienced radiologists is expected to be “gold standard,” however, it is quite time-consuming and not applicable in a large database.⁵⁵ Automatic and semiautomatic methods performed better when there are great differences between the lesion and background, and both methods have been developed to improve the accuracy in recent decades.⁵⁶

Radiomics features extracted from images are divided into shape, intensity, texture, gradient, wavelet features, and many more. We introduced the most common features that applied in study researches. Shape features are based on the reconstructed 3-dimensional images to assess the geometric characteristics.⁵⁵ Parameters from these features include volume, the surface-to-volume ratio, shape, and compactness which are regarded as vital features to evaluate the characteristics of tumors.⁵⁷ For example, with the same volume, a speculated lesion has a higher surface-to-volume ratio compared to a round one, which is more probably to be malignant.⁵⁷ Although shape can be transformed into a quantitative feature, it is not a specific indicator to distinguish the malignant lesions from benign ones. First-order statistics are dependent on a single-pixel intensity value rather than relationship between neighboring pixels. Tumor intensity histogram-based features are known as the first-order features which include mean, median, standard deviation, kurtosis, skewness, energy, entropy, uniformity, and variance.⁵⁷ These features are used to predict the prognosis in the machine learning framework. For example, kurtosis is a measure of whether data are distributed normally. Invasive tumors are composed of more heterogenous tissues that might be reflected by pixel values.²² Texture-based features are known as second-order statistics and used widely in radiomics analysis to evaluate the intertumoral heterogeneity. It has the ability to distinguish the pixels at different spacing and angles at adjacent or nearest-neighbor pixels calculated by using spatial gray-level dependence matrices.³⁶ Considering spatial relationships, texture features are divided into gray-level co-occurrence matrix (GLCM),⁵⁸ gray-level run length matrix,⁵⁹ gray-level size zone matrix,⁶⁰ and the neighborhood gray-level size zone matrix.⁶¹ Wavelet features are filter transforms containing the intensity and textural information and regarded as higher order statistic.⁶² It shows the spatial relationship among 3 or more pixels. For example, Gabor and Fourier extract spatial or spatial-temporal features, while Co-occurrence of Local Anisotropic Gradient Orientations extract the image voxel an entropy value related to the co-occurrence matrix of gradient orientations.^{63,56} Some of these features extracted from region of interest (ROI) may be redundant for a specific task, therefore selecting useful information by using machine algorithms is important in radiomics analysis. Machine learning algorithms include decision trees and random forests, support vector machines, deep neural networks, and so on.⁵⁶ Then the selected features, with reproductive,

Table 1. Studies on Differentiating Between Malignant and Benign Breast Lesions.

First Author, Year	Study Design	Number of Patients	MRI Modality	Magnetic Field	Radiomics Features	Outcomes
Bahreini et al (2010) ⁶	Retrospective	60	DCE-MRI	1.5 T	Contour signature, Fourier descriptor, Fourier factor.	The first classifier achieved an AUC of 0.82, specificity of 60% at sensitivity of 81%. The second classifier achieved an AUC of 0.90, specificity of 79% at sensitivity of 81%.
Bickelhaupt et al (2108) ⁷	Retrospective	222	DWI-MRI	1.5 T	First order statistics, volume features, shape features, texture features.	The radiomics feature model reduced false-positive results from 66 to 20 (specificity 70.0%) at the predefined sensitivity of greater than 98.0% in the independent test set, with BI-RADS 4a and 4b lesions benefiting from the analysis (specificity 74.0%; 60.0%) and BI-RADS 5 lesions showing no added benefit.
Bickelhaupt et al (2017) ⁸	Prospective	50	T2WI, DWI, DWIBS	1.5 T	First-order features, volume features, shape features, texture features.	Radiomic classifiers consisted of 11 parameters achieved AUC of 84.2%/85.1%, compared to 77.4% for mean ADC and 95.9%/95.9% for the experienced radiologist using ceMRI/ueMRI.
Holli et al (2010) ⁹	Retrospective	20	DCE-MRI	1.5 T	Texture features.	All classification methods employed were able to differentiate between cancer and healthy breast tissue and also invasive lobular and ductal carcinoma with classification accuracy varying between 80% and 100%.
Hu et al (2018) ¹⁰	Retrospective	88	DCE-MRI	3.0 T	Tumor size, shape, first-order statistics of descriptor values and high-order texture features.	The area under the ROC curve of the prediction model comprising ADC radiomic features was 0.79 when the cutoff value was 0.45, and the accuracy, sensitivity, and specificity were 80.0%, 0.813, and 0.778.
Jiang et al (2018) ¹¹	Retrospective	205	DCE-MRI, DWI-MRI	1.5 T	Texture and morphology features.	By using 10-fold cross-validation scheme, combined morphological and kinetic features achieved a diagnostic average accuracy of 0.87.
Karahaliou et al (2010) ¹²	Not mentioned	82	DCE-MRI	1.5 T	Texture features (GLCM).	Selected texture features extracted from the signal enhancement ratio map achieved an area under receiver operating characteristic curve of 0.922 ± 0.029 , a performance similar to postinitial enhancement map features (0.906 ± 0.032) and statistically significantly higher than for initial enhancement map (0.767 ± 0.053) and first postcontrast frame (0.756 ± 0.060) features.
Nie et al (2008) ¹³	Retrospective	71	T1-weighted 3D SPGR (RF-FAST)	1.5 T	Morphological parameters and GLCM texture features	The ACU was 0.86.
Whitney et al (2019) ¹⁴	Retrospective	338	DCE-MRI	1.5 T/ 3.0 T	Size, shape, morphology, texture enhancement, and kinetic curve assessment and enhancement variance kinetics	Their differences in AUC-ROC by biopsy condition failed to reach statistical significance, but we were unable to prove equivalence using a margin of $\Delta\text{AUC-ROC} = 0.10$.
Gibbs and Turnbull (2003) ¹⁵	Retrospective	79	DCE-MRI	1.5 T	Texture features	On combining features obtained using textural analysis with lesion size, time to maximum enhancement, and patient age, a diagnostic accuracy of $Az = 0.92 \pm 0.05$ was demonstrated.

Abbreviations: ADC, apparent diffusion coefficient; AUC, area under the curve; BI-RADS, Breast Imaging Reporting and Data System; ceMRI, contrast enhanced magnetic resonance imaging; GLCM, gray-level co-occurrence matrix; MRI-DCE, dynamic contrast-enhanced; DWI, diffusion-weighted imaging; DWIBS, DWI with background suppression; MRI, magnetic resonance imaging; ROC, receive operating characteristics; T2WI, T2-weighted image; ueMRI, unenhanced magnetic resonance imaging; 3D-SPGR (RF-FAST), 3-dimensional SPGR(RF-FAST).

informative, and nonredundant characteristics, are used to evaluate the associations with clinical outcomes.

The Application of Radiomics

Role of MRI

Magnetic resonance imaging of breast is widely applied in screening in high risk women, staging, evaluating curative effect, monitoring recurrence, especially providing complementary information for uncertain findings on mammography and ultrasonography. In recent years, diffusion-weighted imaging (DWI) and dynamic contrast-enhanced (DCE) have been

used to provide functional features of breast lesions to assess precise diagnosis. Diffusion-weighted imaging, known as a contrast-free protocol, has been shown promise in the diagnosis of breast cancer.⁶⁴ It can reflect tissue microenvironment and membrane integrity through depicting the diffusivity of the tissues.⁶⁵ Changes of water diffusion in tissues are associated with pathological processes that can be calculated as apparent diffusion coefficient (ADC).⁶⁶ Previous studies have investigated that DWI hold potentials to improve the detection and biological characterization of breast cancer.⁶⁷⁻⁶⁹ Based on DWI, several advanced modelling approaches have been evaluated to characterize structural anisotropy (diffusion tensor

Table 2. Studies on Prediction of Axillary Lymph Node Metastasis.

First Author, Year	Study Design	Number of Patients	MRI Modality	Magnetic Field	Radiomics Features	Outcomes
Chai <i>et al</i> (2019) ¹⁶	Retrospective	120	DCE-MRI	3.0 T	Morphological and texture features.	The accuracy/AUC of the 4 sequences was 79%/0.87, 77%/0.85, 74%/0.79, and 79%/0.85 for the T1WI, CE2, T2WI, and DWI, respectively. When CE2 was augmented by adding kinetic features, the model achieved the highest performance (accuracy = 0.86 and AUC = 0.91).
Cui <i>et al</i> (2019) ¹⁷	Retrospective	102	DCE-MRI	3.0 T	Morphological, NGLDM, GLRLM, GLCM, GLGCM, Tamura, and grayscale histogram features.	The SVM classifier performed best, with the highest accuracy of 89.54%, and obtained an AUC of 0.8615 for identifying the lymph node status.
Dong <i>et al</i> (2018) ¹⁸	Retrospective	146	T2FS, DWI	1.5 T	Nontexture and texture parameter features.	Model of T2-FS yielded the highest AUC of 0.847 in the training set and 0.770 in the validation set. Model of DWI reached the highest AUC of 0.847 in the training set and 0.787 in the validation set. Combination of T2-FS and DWI features yielded an AUC of 0.863 in the training set and 0.805 in the validation set.
Han <i>et al</i> (2019) ¹⁹	Retrospective	411	DCE-MRI	1.5 T	Shape features, first-order features, textural features	The AUC of radiomic signature was 0.76 and 0.78 in training and validation cohorts, respectively. Another radiomic signature was constructed to distinguish the number of metastatic LNs, which also showed moderate performance (AUC = 0.79).
Liu <i>et al</i> (2019) ²⁰	Retrospective	163	DCE-MRI	1.5 T	Shape features, histogram features, texture features, and Laws features.	In the independent validation set, combining radiomics features and clinicopathologic characteristics, AUC was 0.869. Using radiomic features alone in the same procedure, the validation set AUC was 0.806.
Liu <i>et al</i> (2019) ²¹	Prospective	149	DCE-MRI	1.5 T/3.0 T	First-order statistics, shape- and size-based features, wavelet-based features, and texture-based features.	The value of AUC for a combined model (0.763) was higher than that for MRI ALN status alone (0.665; $P = .029$) and similar to that for the radiomics signature (0.752; $P = .857$).

Abbreviations: ALN, axillary lymph node; AUC, area under the curve; CE2, second postcontrast phase; DCE, dynamic contrast-enhanced; DWI, diffusion-weighted imaging; GLCM, gray-level co-occurrence matrix; GLRLM, gray-level run length matrix; LNs, lymph nodes; MRI, magnetic resonance imaging; SVM, support vector machine; T1WI, T1-weighted image; T2-FS, T2-weighted fat suppression; T2WI, T2-weighted image; NGLDM, Neighboring Gray-Level Dependence Matrix; GLGCM, Gray Level-Gradient Co-occurrence Matrix.

imaging [DTI]), microvasculature (intravoxel incoherent motion [IVIM]), and microstructural complexity (diffusion kurtosis imaging) for better diagnosis of breast cancer.⁶⁶ Diffusion kurtosis imaging extends standard DWI to assess anisotropic details of water diffusion.⁷⁰ Mean diffusivity and fractional anisotropy are parameters of DTI to reflect the average anisotropy and the degree of anisotropy.⁷¹ Intravoxel incoherent motion aims to evaluate tissue diffusivity and tissue microcapillary perfusion at once based on biexponential model.⁷² The following parameters are commonly used: true molecular diffusion (D or D_t), perfusion-related diffusion (D^* , D_p , or D_f), and perfusion fraction (f , f_p , or f_{IVIM}).⁷³ Diffusion kurtosis imaging quantifies non-Gaussianity of the water displacement distribution⁶⁶ and has a higher sensitivity and specificity in cancer detection than ADCs.⁶⁵ DCE is a contrast-enhanced protocol with excellent sensitivity for the detection of breast cancer and provides functional information about neoangiogenesis as a specific feature of tumor.⁷⁴ The sensitivities of detecting invasive cancers by using DCE-MRI are more than 90%, while the specificities range from 20% to 100%.^{75,76} In addition, the enhancement patterns of benign lesions were overlapped with malignant lesions.⁷⁷ By using conventional imaging technologies, the diagnostic value is mostly depended

on experienced radiologists. Thus radiomics with high diagnostic accuracy and applicable value deserves to be evaluated.

Compared to mammography and US, MRI plays an important role in the diagnosis of breast cancer. First, MRI has a higher resolution of soft tissues, which is more sensitive to detect masses.⁷⁸ Second, MRI can provide information about the anatomy of the bilateral breast, the relationship between the tumor and surrounding tissue, and lymph node (LN) status. Third, different sequences of MRI could provide functional information of tumors, such as blood flow and breast density, and find the heterogeneity of tumor microenvironments. Fourth, due to the technological limitation of mammography, MRI improves the variations in breast symmetry and masking effect to detect cancer in dense breasts. By using hand-held US, the image quality is mostly dependent on skilled and qualified doctors, while MRI could provide more standard and comprehensive images.

Reliable Differentiation Between Malignant and Benign Breast Lesions

Precise diagnosis for differentiating between malignant and benign breast lesions is necessary for follow-up treatment options. The treatment decisions make a little different, with

Table 3. Studies on Predicting Molecular Subtypes of Breast Cancer.

First Author, Year	Study Design	Number of Patients	MRI Modality	Magnetic Field	Radiomics Features	Studies Directions	Outcomes
Kirsi Holli-Helenius <i>et al</i> (2017) ²²	Not mentioned	27	DCE-MRI, DWI-MRI	1.5 T	Texture features	To assist in differentiating estrogen receptor (ER) positive breast cancer molecular subtypes.	The 2 most discriminative texture parameters to differentiate luminal A and luminal B subtypes were sum entropy and sum variance ($P = .003$). The AUCs were 0.828 for sum entropy ($P = .004$), 0.833 for sum variance ($P = .003$), and 0.878 for the model combining texture features sum entropy, sum variance ($P = .001$).
Fan <i>et al</i> , (2018) ²³	Retrospective	77	DCE-MRI	3.0 T	Texture features (GLCM)	To predict the Ki-67 status of patients with estrogen receptor (ER)-positive breast cancer.	Multivariate analysis showed that features from the tumor subregions associated with early TTP yielded the highest performance (AUC = 0.807) among the subregions for predicting the Ki-67 status.
Fan <i>et al</i> (2017) ²⁴	Retrospective	60	DCE-MRI	1.5 T	First-order statistics, texture features.	Prediction of the molecular subtypes of breast cancer.	The predictive model discriminated among the luminal A, luminal B, HER2, and basal-like subtypes, with AUC values of 0.867, 0.786, 0.888, and 0.923.
Fan <i>et al</i> (2019) ²⁵	Retrospective	211	DCE-MRI	3.0 T	Texture features	To predict the molecular subtypes of breast cancer.	The tumor subregion related to fast-flow kinetics showed the best performance among the subregions for differentiating between patients with 4 molecular subtypes (AUC = 0.832).
Grimm <i>et al</i> (2015) ²⁶	Retrospective	275	T1WI, T2-FS	1.5 T/3.0 T	Size, shape, gradient, texture, and dynamic features.	To characterize the relationship between breast MRI and molecular subtype.	The imaging features were associated with both luminal A and luminal B molecular subtypes. No association was found for either HER2 or basal molecular subtype and the imaging features.
Juan <i>et al</i> (2018) ²⁷	Retrospective	159	DCE-MRI	3.0 T	Morphological features, gray-scale histograms and texture features.	To investigate the association between Ki-67 expression and radiomics features in patients with invasive breast cancer.	One morphology metric (area), 3 gray-scale histogram indexes (standard deviation, skewness and kurtosis) and 3 texture features (contrast, homogeneity and inverse differential moment) demonstrated a significant difference.
Ko <i>et al</i> (2016) ²⁸	Not mentioned	75	DCE-MRI	1.5 T	Texture features.	To investigate whether texture analysis of magnetic resonance images correlates with histopathological findings	High histologic grades showed increased uniformity and decreased entropy on contrast-enhanced T1-weighted subtraction images, whereas the opposite tendency was observed on T2-weighted images.
Liang <i>et al</i> (2018) ²⁹	Retrospective	318	T2WI, T1 + C	1.5 T	Intensity, shape, texture, and wavelet features.	To predict the Ki-67 status in patients with breast cancer.	The T2WI-based radiomics classifier exhibited good discrimination for Ki-67 status, with areas under the receiver operating characteristic curves of 0.762 (95% CI: 0.685-0.838) and 0.740 (95% CI: 0.645-0.836) in the training and validation data sets.
Ma <i>et al</i> (2018) ³⁰	Retrospective	377	DCE-MRI	3.0 T	Morphological, gray scale statistic, and texture features.	To investigate whether quantitative radiomics features are associated with Ki67 expression of breast cancer.	The model that used naive Bayes classification method achieved the best performance than the other 2 methods, yielding 0.773 AUC, 0.757 accuracy, 0.777 sensitivity, and 0.769 specificity.
Monti <i>et al</i> (2018) ³¹	Not mentioned	49	DCE-MRI	3.0 T	Shape features	To build predictive models for the discrimination of molecular receptor status (ER+/ER-, PR+/PR-, and HER2+/HER2-), TN/ nontriple negative (NTN), ki67 levels, and tumor grade.	The predictive model coefficients were computed for each classification task. The AUC values obtained were 0.826 ± 0.006 for ER+/ER-, 0.875 ± 0.009 for PR+/PR-, 0.838 ± 0.006 for HER2+/HER2-, 0.876 ± 0.007 for TN/NTN, 0.811 ± 0.005 for ki67 + /ki67-, and 0.895 ± 0.006 for low grade/high grade.
Saha <i>et al</i> (2018) ³²	Not mentioned	922	DCE-MRI	1.5 T/3.0 T	Texture features	To investigate features published in the literature as well as those developed in laboratory to find the association between molecular subtype and features.	Multivariate models were predictive of luminal A subtype with AUC = 0.697, triple-negative breast cancer with AUC = 0.654, ER status with AUC = 0.649 (95% CI: 0.591-0.705).

(continued)

Table 3. (continued)

First Author, Year	Study Design	Number of Patients	MRI Modality	Magnetic Field	Radiomics Features	Studies Directions	Outcomes
Sun <i>et al</i> (2018) ³³	Retrospective	107	Axial fast spin echo (FSE) T1WI, T2WI-FS, DWI	1.5 T/3.0 T	Texture features	To investigate the molecular subtypes of breast cancer.	The differentiation accuracies of Fisher discriminant analysis on the enhanced high-resolution T1WI were 82.8% and 86.4% for 1.5 T and 3.0 T imaging. Fisher discriminant analysis on DWI texture features were achieved with a classification ability of 73.4% and 88.6%. The combined discriminant results for 2 kinds of magnetic resonance images were 95.0%, 97.7% in 1.5 T, and 3.0 T imaging, respectively.
Wang <i>et al</i> (2015) ³⁴	Not mentioned	88	DCE-MRI	3.0 T	Morphologic, densitometric, and statistical texture measures of enhancement	To determine the added discriminative value of detailed quantitative characterization of background parenchymal enhancement in addition to the tumor itself on DCE-MRI in identifying TN breast cancer.	Imaging features based on the tumor region achieved an AUC of 0.782 in differentiating triple-negative cancers from others, in line with the current state of the art. When background parenchymal enhancement features were included, the AUC increased significantly to 0.878 ($P < .01$).
Xie <i>et al</i> (2019) ³⁵	retrospective	134	DCE-MRI, DWI-MRI	3.0 T	Histogram analysis	To identify TN breast cancer imaging biomarkers in comparison to other molecular subtypes using multiparametric MR imaging maps and whole tumor histogram analysis.	The significant parameters on the univariate analysis achieved an AUC of 0.710 with a sensitivity of 63.6% and a specificity of 73.1% at the best cutoff point for differentiating TN cancers from luminal A cancer. An AUC of 0.763 (95% CI: 0.608-0.917) with a sensitivity of 86.4% and a specificity of 72.2% was achieved for differentiating TN cancers from HER2 positive cancers. Also, an AUC of 0.683 with a sensitivity of 54.5% and a specificity of 83.9% was achieved for differentiating TN cancers from non-TN cancers.

Abbreviations: AUC, area under the curve; CI, confidence interval; DCE, dynamic contrast-enhanced; DWI, diffusion-weighted imaging; ER+, positive estrogen receptor; ER-, negative estrogen receptor; GLCM, gray-level co-occurrence matrix; HER-2+, positive human epidermal growth factor receptor 2; HER-2-, negative human epidermal growth factor receptor 2; MRI, magnetic resonance imaging; PR+, positive progesterone receptor; PR-, negative progesterone receptor; T2-FS, T2-weighted fat suppression; T2WI, T2-weighted image; TN, triple negative; TTP, time to peak.

Table 4. Studies on Prediction of Tumor Response to Chemotherapy in Breast Cancer.

First Author, Year	Study Design	Number of Patients	MRI Modality	Magnetic Field	Radiomics Features	Studies Directions	Outcomes
Ahmed <i>et al</i> (2013) ³⁶	Retrospective	100	DCE-MRI	3.0 T	Texture features	To predict response to chemotherapy in a cohort of patients with breast cancer.	The selected features showed significant differences between responders and partial responders of chemotherapy.
Braman <i>et al</i> (2017) ³⁷	Retrospective	117	DCE-MRI	1.5 T	First-order statistics, Gabor features, Haralick features, CoLLiAge features	In this study, we evaluated the ability of radiomic textural analysis of intratumoral and peritumoral regions on pretreatment breast cancer DCE-MRI to predict pCR to NAC.	A combined intratumoral and peritumoral radiomic feature set yielded a maximum AUC of 0.78 \pm 0.030 within the training set and 0.74 within the independent testing set. Receptor status-specific feature discovery and classification enabled improved prediction of pCR, yielding maximum AUCs of 0.83 \pm 0.025 within the HR+, HER2- group using DLDA and 0.93 \pm 0.018 within the TN/HER2+ group using a naive Bayes classifier.
Cain <i>et al</i> (2019) ³⁸	Retrospective	288	DCE-MRI	Not mentioned	Texture features	To predict pathologic complete response (pCR) to NAT in patients with breast cancer.	The AUC values for predicting pCR in TN/HER2+ patients who received NAT were significant (AUC = 0.707)
Chamming's <i>et al</i> (2018) ³⁹	Retrospective	85	T1WI, T2WI	1.5 T	Texture features	To evaluate whether texture features of breast cancers were associated with pCR after NAC.	T1-weighted kurtosis showed good performance for the identification of triple-negative breast cancer (AUC = 0.834).
Fan <i>et al</i> (2017) ⁴⁰	Retrospective	57	DCE-MRI	1.5 T/3.0 T	Morphologic features, texture features, first-order statistical features and dynamic features.	To predict NAC in breast cancer.	The classifier based on the features yield a LOOCV-AUC of 0.910 and 0.874 for the main and the reproducibility study cohort.
Henderson <i>et al</i> (2017) ⁴¹	Not mentioned	88	T2WI	3.0 T	Texture features	To investigate whether interim changes in heterogeneity (measured using entropy features) were associated with pathological residual cancer burden in patients receiving NAC for primary breast cancer.	Association of ultimate pCR with coarse entropy changes between baseline/interim MRI across all lesions yielded 85.2% accuracy (area under ROC curve: 0.845). Excellent sensitivity/specificity was obtained for pCR prediction within each immunophenotype: ER+: 100%/100%; HER2+: 83.3%/95.7%, TNBC: 87.5%/80.0%.
Liu <i>et al</i> (2019) ⁴²	Retrospective	586	T2WI, DWI, T1 + C	Not mentioned	Shape- and size-based features; first 2 order statistical features; textural features; wavelet features.	To predict pCR to NAC in breast cancer.	Radiomic signature combining multiparametric MRI achieved an AUC of 0.79
Michoux <i>et al</i> (2015) ⁴³	Not mentioned	69	T2-WI, DWI, 3D gradient echo axial T1-weighted sequence with fat suppression (SPAIR).	1.5 T	Texture features	To predict tumor response to NAC in breast cancer.	A model based on 4 pre-NAC parameters (inverse difference moment, GLN, LRHGE, washin) and k-means clustering as statistical classifier identified nonresponders with 84% sensitivity.
Panzeri <i>et al</i> (2018) ⁴⁴	Not mentioned	69	DWI-MRI, DCE-MRI	Not mentioned	First-order texture kinetics	To assess correlations between volumetric first-order texture parameters on baseline MRI and pathological response after NAC for locally advanced breast cancer.	Higher levels of AUC max (P value = .0338), AUC range (P value = .0311) and TME75 (P value = .0452) and lower levels of washout 10 (P value = .0417), washout 20 (P value = .0138), washout 25 (P = .0114), washout 30 (P value = .05) were predictive of noncomplete response.

(continued)

Table 4. (continued)

First Author, Year	Study Design	Number of Patients	MRI Modality	Magnetic Field	Radiomics Features	Studies Directions	Outcomes
Tenel <i>et al</i> (2014) ⁴⁵	Retrospective	58	DCE-MRI	3.0 T	Texture features	To investigate the potential of texture analysis to predict the clinical and pathological response to NAC in patients with locally advanced breast cancer (LABC) before NAC is started.	The most significant feature yielding an area under the curve (AUC) of 0.77 for response prediction for stable disease versus complete responders after 4 cycles of NAC.
Wu <i>et al</i> (2016) ⁴⁶	Not mentioned	35	DCE-MRI	3.0 T	Texture features	To predict pathological response of breast cancer to NAC.	In multivariate analysis, the proposed imaging predictors achieved an AUC of 0.79 ($P = .002$) in leave-one-out cross-validation. This improved upon conventional imaging predictors such as tumor volume (AUC = 0.53) and texture features based on whole-tumor analysis (AUC = 0.65)
Banerjee <i>et al</i> (2018) ⁴⁷	Retrospective	96	DCE-MRI	Not mentioned	Riesz, first-order statistical features, gray-level co-occurrence	To predict treatment response, specifically the residual tumor (RT) status and pathological complete response (pCR), in response to neoadjuvant chemotherapy.	The most efficient models are based on first-order statistics and Riesz wavelets, which predicted RT with an AUC value of 0.85 and pCR with an AUC value of 0.83, improving results reported in a previous study by approximately 13%.

Abbreviations: ADC, apparent diffusion coefficient; AUC, area under the curve; CoLIAGe, Co-occurrence of Local Anisotropic Gradient Orientations; DCE, dynamic contrast-enhanced; DWI, diffusion-weighted imaging; ER, estrogen receptor; HER-2, human epidermal growth factor receptor 2; MRI, magnetic resonance imaging; NAC, neoadjuvant chemotherapy; NAT, neoadjuvant therapy; pCR, pathological complete response; PR, progesterone receptor; ROC, receive operating characteristics; TN, triple negative; T1WI, T1-weighted image; T2WI, T2-weighted image; HR+, hormone receptor positive; LOOCV, leave-one-out cross-validation; TNBC, triple negative breast cancer; GLN, Gray-Level Nonuniformity; LRHGE, Long Run High Gray-Level Emphasis; LABC, locally advanced breast cancer.

Table 5. Studies on Prediction of Survival Outcomes in Patients With Breast Cancer.

First Author, Year	Study Design	Number of Patients	MRI Modality	Magnetic Field	Radiomics Features	Studies Directions	Outcomes
Kim <i>et al</i> (2017) ⁴⁸	Retrospective	203	DCE-MRI	1.5 T	Texture features	To determine the relationship between tumor heterogeneity assessed by means of MRI texture analysis and survival outcomes in patients with primary breast cancer.	In multivariate analysis, a higher N stage (RFS hazard ratio, 11.15 (N3 stage); $P = .002$, Bonferroni adjusted $\alpha = 0.0167$), triple-negative subtype (RFS hazard ratio, 16.91; $P = .001$, Bonferroni adjusted $\alpha = 0.0167$), high risk of T1 entropy (less than the cutoff values (mean, 5.057; range, 5.022-5.167], RFS hazard ratio, 4.55; $P = .018$), and T2 entropy (equal to or higher than the cutoff values (mean, 6.013; range: 6.004-6.035), RFS hazard ratio = 9.84; $P = .001$) were associated with worse outcomes. The ROC curves of the model yielded AUC values of 0.88, 0.77 and 0.73, for the training, leave-one-out cross-validated and bootstrapped performances, respectively.
Chan <i>et al</i> (2017) ⁴⁹	Retrospective	563	DCE-MRI	1.5 T	Not mentioned	We present a radiomics model to discriminate between patients at low risk and those at high risk of treatment failure at long-term follow-up based on eigentumors.	
Drukker <i>et al</i> (2018) ⁵⁰	Not mentioned	162	DCE-MRI	1.5 T	Not mentioned	To predict recurrence-free survival “early on” in breast cancer neoadjuvant chemotherapy.	The C-statistics for the association of METV with recurrence-free survival were 0.69 with 95% confidence interval of 0.58-0.80 at pretreatment and 0.72 (0.60-0.84) at early treatment. The hazard ratios calculated from Kaplan-Meier curves were 2.28 (1.08-4.61), 3.43 (1.83-6.75), and 4.81 (2.16-10.72) for the lowest quartile, median quartile, and upper quartile cutpoints for METV at early treatment.
Park <i>et al</i> (2018) ⁵¹	Retrospective	294	DCE-MRI	1.5T	Morphological, histogram-based features, and higher-order texture features.	To develop a radiomics signature to estimate DFS in patients with invasive breast cancer and to establish a radiomics nomogram that incorporates the radiomics signature and MRI and clinicopathological findings.	The radiomics nomogram estimated DFS (C-index, 0.76; 95% confidence interval (CI): 0.74-0.77) better than the clinicopathological (C-index, 0.72; 95% CI: 0.70-0.74) or Rad-score only nomograms (C-index, 0.67; 95% CI, 0.65-0.69).
Pickles <i>et al</i> (2016) ⁵²	Retrospective	112	DCE-MRI	3.0 T	Texture, shape features	To determine if associations exist between pretreatment DCE-MRI and survival intervals and compare the prognostic value of DCE-MRI parameters against traditional pretreatment survival indicators.	Accuracy of risk stratification based on either traditional (59%) or DCE-MRI (65%) survival indicators performed to a similar level. However, combined traditional and MR risk stratification resulted in the highest accuracy (86%).

Abbreviations: AUC, area under the curve; CI, confidence interval; DCE, dynamic contrast-enhanced; DFS, disease-free survival; MRI, magnetic resonance imaging; ROC, receive operating characteristics; RFS, recurrence-free survival; METV, the most enhancing tumor volume.

follow-up for likely benign lesions or surgery for likely malignant lesions. Recent studies suggested that radiomics analysis could provide promising conclusions for the diagnosis of breast cancer and a better discrimination ability than conventional parameters (Table 1).⁶⁻¹⁵ From the included studies in Table 1, area under the curve (AUC) of radiomics models could achieve 0.79 to 0.92, with good performance in differentiating malignant lesions from benign ones. DCE and DWI are the most common modalities for radiomics analysis. Bickelhaupt *et al*⁷ conducted a retrospective study extracting first-order statistics, volume, shape, and texture features from DWI-MRI imaging and suggested that the radiomics model (AUC = 0.91) performed better than other models, including ADC median (AUC = 0.84) and apparent kurtosis coefficient median (AUC = 0.87), moreover greatly increased the sensitivity and specificity of differentiating the malignant lesions from benign ones. However, another study further compared the diagnostic accuracy between radiomics and experienced radiologists.⁸ The results showed that by using unconstrained and constrained MRI, expert radiologists (AUC = 0.959/0.959) performed better than radiomics models (AUC = 0.842/0.851). The performance of radiomics was desirable to reach highly experienced radiologists in further studies. Holli *et al*⁹ investigated the texture features to distinguish healthy breast tissue and breast cancer through DCE-MRI. The image selection of DCE-MRI was from T1-weighted precontrast, 2 contrast-enhanced series (contrast first and contrast last) and their subtraction series (subtraction first and subtraction last). The classification accuracy of different breast tissues by using texture features from subtracted images was 100%. Another interesting study based on DCE extracted features from initial enhancement, postinitial enhancement, and signal enhancement ratio (SER) parametric maps for texture analysis.¹² Compared to the initial enhancement map (AUC = 0.767), the SER map (AUC = 0.92) and postinitial enhancement map (AUC = 0.906) achieved better performance. Based on DCE and DWI modalities, Xinhua Jiang *et al*¹¹ found the multivariate models, combining morphological and kinetic parameters and ADC values, increased the overall accuracy to 0.90. Some researchers found that background parenchymal enhancement (BPE), which was known as normal breast tissue enhancement on DCE-MRI, could negatively affect the impact of a correct radiological diagnosis in MRI. It might cause increased omission diagnostic rate by obscuring malignancy or increased false-positive rates by mimicking the appearance of breast cancer.^{79,80} However, L. Losurdo *et al*⁸¹ explored some statistical measurements based on full automatized analysis to identify abnormal breast tissue based on BPE to improve diagnostic accuracy for radiologists. In conclusion, radiomics performed high value on the differentiation between malignant and benign breast lesions and increased the sensitivity and specificity of disease diagnosis. In addition, microcalcification is regarded as one of the main indirect signs of malignant lesions.⁸² Multiscale texture analysis for microcalcification diagnosis on mammography to distinguish normal/abnormal (AUC = 98.46%) and benign/malignant (AUC = 94.19%) achieved excellent results.⁸³

However, studies of radiomics focused on microcalcification of MRI need to be evaluated in further research.

Prediction of Axillary Lymph Node Metastasis

The status of axillary LN of patients with breast cancer remains an important role for staging and prognosis. Accurate diagnosis of axillary lymph node metastasis (ALNM) can provide vital information for clinicians to make follow-up treatment plans. The gold standard of confirming ALNM status in breast cancer cases is axillary lymph node dissection (ALND) that is regarded as a surgical process to assess ALN status.⁸⁴ According to the American Society for Clinical Oncology guidelines and another randomized clinical trial reports, early stage breast cancer with 1 or 2 sentinels lymph node metastasis (LNM) should not take ALND that may cause a significant overtreatment.^{85,86} The sentinel LN is the first site to receive lymphatic drainage from primary tumors, thus sentinel LN biopsy (SLNB) can provide valuable information to guide the follow-up treatment. Therefore, SLNB is used as an alternative method of ALND for patients with early stage breast cancer to predict LNM status with high accuracy. However, both SLNB and ALND are invasive method that may cause potential complications, such as lymphedema, dysfunction of sense, pain, nerve injury, and so on.⁸⁴

Conventional imaging examinations to predict LNM is a helpful method to improve accuracy, however, their abilities are limited still with a high false-negative rate. Recent studies investigated that radiomics features to predict LNM greatly improved the accuracy and AUC (Table 2).¹⁶⁻²¹ From the included studies in Table 2, AUC of radiomics models could achieve 0.74 to 0.91, with good performance in predicting LN status. Adding clinical features to the radiomics models, the diagnostic value and AUC of combined models could increase a lot.^{19,20} Chai *et al*¹⁶ compared 4 different sequences of MRI including T1-weighted image (T1WI), T2-weighted image (T2WI), DCE-MRI, and DWI-MRI to find out the best modalities in predicting LN status for clinical practice. The results showed based on morphological and texture features, the second postcontrast phase (CE2) of DCE and the contrast enhancement kinetic features achieved a better performance than others (AUC = 0.91), while radiomics features extracted from other sequence did not outperform the combined models (AUC_{T1WI} = 0.87, AUC_{CE2} = 0.85, AUC_{T2WI} = 0.79, AUC_{DWI} = 0.85). It is interesting to find that all the features combined from 4 sequences adding kinetics, the diagnostic performance was not differentiated ($P = .48$). While Dong *et al*¹⁸ compared 2 radiomics models based on T2-weighted fat suppression (T2-FS) and DWI, the performance to distinguish LNM status of both models was satisfied and the diagnostic value was not different between 2 models (for training set: AUC_{T2-FS} = 0.847, AUC_{DWI} = 0.847; for validation set: AUC_{T2-FS} = 0.770, AUC_{DWI} = 0.787). Most studies concentrated on intratumoral regions, however, peritumoral features have also showed an association with LN status in the predictive models.²⁰ Further researches focused on the value of peritumoral features should

be evaluated. Radiomics was used as a noninvasive and highly accurate method based on mathematical models to predict ALNM and help clinicians to make therapeutic regimens for patients.

Predicting Molecular Subtypes of Breast Cancer

Molecular subtypes of breast cancer were divided into 4 categories based on hormone status by immunohistochemical (IHC) analyses: luminal A, luminal B, human epidermal growth factor receptor 2 (HER2) overexpressing, and triple negative (TN). Cases with positive estrogen receptor (ER+) and/or positive progesterone receptor (PR+), negative expression of HER2, and Ki67 <14% were categorized as luminal A breast cancer, which has a best prognosis.⁸⁷⁻⁸⁹ Cases with ER (+) and/or PR (+), HER-2 (-), and Ki67 \geq 14% or ER (+) and/or PR (+), HER2 (+) were categorized as luminal B breast cancer, which had high-grade tumors and higher proliferation.^{87,89} Cases with ER (-), PR (-), and HER2 (+) were classified as HER2-overexpressing breast cancer, which has a poorer prognosis than luminal breast cancers.⁸⁷⁻⁸⁹ Cases with ER (-), PR (-), and HER2 (-) were classified as TN breast cancer, which has the poorest survival rate and is related to LN involvement.^{87,89,90} The various subtypes have been widely used and involved in treatment planning. However, the molecular subtype is confirmed by IHC analyses on sample tissues that may not reflect the complexity and heterogeneity of whole tumor. Previous studies evaluated the association between MRI features with molecular subtypes, however, the results have not come to a consistent conclusion.^{91,92} Different subtypes of breast cancer have their own biological characteristics that can be reflected on the image. For example, HER2-overexpressing subtype was associated with an overexpression of vascular endothelial growth factor, which can increase angiogenesis.⁹³ HER2-overexpressing breast cancer had a higher enhancement value than other subtypes that could be assessed from radiomic features. In recent years, radiomics analyses have been used to predict the molecular subtypes of breast cancer in many studies, and it can be used as a potential biomarker to differentiate the subtypes of breast cancer with good performance (AUC = 0.74 – 0.92; Table 3)²²⁻³⁵. Fan *et al*²⁴ obtained radiomics features and dynamic features from DCE-MRI as well as 2 clinical information to get a predictive model to distinguish luminal A, luminal B, HER2-overexpressing, and TN. By using 24 features, the AUC values were 0.867, 0.786, 0.888, and 0.923, respectively. In this study, the luminal A cancer had low kurtosis and skewness that were related to heterogeneity. High values of these features were also found to be associated with the poor response of treatment in other types of tumors.⁹³⁻⁹⁵ It was consistent with another study that high-ki67 lesions tended to have higher kinetics.³⁰ Another study found that texture features extracted from a quantitative ADC map and DCE maps (washin and washout) had the ability to identify triple negative breast cancer (TNBC) based on histogram analysis.³⁵ The models achieved an AUC of 0.710 (TNBC vs luminal A), 0.763 (TNBC vs HER2 positive), and 0.683 (TNBC vs non-

TNBC). Intratumoral necrosis was dominant in TNBC, therefore the parameters related to washin were significantly lower compared to other types.

Although DCE-MRI has been used widely in the classification of breast cancer, a problem was found that a certain voxel may reflect various kinetics features due to biological characteristics. Previous studies evaluated the image decomposition methods to identify intratumoral vascular heterogeneity that was proved to be advantageous.^{23,25,96,97} Recent studies also investigated intratumor imaging heterogeneity by using new algorithm to separate tumors with varied enhancement patterns for better classification of breast cancer. Fan *et al*²⁵ conducted a new algorithm (convex analysis of mixture) to separate tumors with varied enhancement patterns. The results found that analysis of subregions had an improved performance than the entire tumor. The present studies aimed to evaluate the potential association between molecular subtypes and radiomics features from MRI and we found the results were promising in the performance of classification. Further efforts are need before these radiomics models can be used to predict histopathological characteristics clinically.

Prediction of Tumor Response to Chemotherapy in Breast Cancer

Patients with advanced stage breast cancer are treated with neoadjuvant chemotherapy (NAC) to reduce the size of tumors before surgery in clinical practice. Considering the tumor response to NAC, breast-conserving surgery may replace mastectomy which can improve the life quality of patients.⁹⁸ However, the heterogeneity of tumors contributed to different responses to NAC, as some cases are insensitive to chemotherapy.⁹⁹ Pathological examinations were the gold standard for the assessment of treatment outcomes, and a pathological complete response (pCR) was associated with a long-time survival benefit.¹⁰⁰ Response Evaluation Criteria in Solid Tumors guidelines based on the measurements of tumor size from imaging data have been used widely to evaluate the efficiency of chemotherapy, however, it could not reflect the complexity of biological progress.¹⁰¹ Therefore, a predictive and accurate marker is expected to be applied in adjusting therapeutic strategies for clinicians and avoiding unnecessary treatment and reducing economic burden for patients. In recent years, some studies reported that radiomics characteristics of MRI were associated with tumor response to chemotherapy and provided great clinical benefits (Table 4).³⁶⁻⁴⁷ In the included literatures, DCE had been used more frequently (9/12) than DWI (3/12) to assess response to NAC. Dynamic contrast-enhanced-MRI can provide the tumor's kinetic characteristics of the contrast agent by producing pharmacokinetic maps. Based on quantitative, multiregion analysis that identified enhancement characteristics, the proposed imaging predictors achieved a better performance (AUC = 0.79) than conventional imaging predictors (AUC = 0.53) and texture features on whole tumor analysis (AUC = 0.65).⁴⁶ However, the problem that extracting post-contrast images at which time points remains ambiguous.

Ahmed *et al*³⁶ found that more textural features were significantly different around the 1 to 3 minutes postcontrast time points between groups (based on response, nodal status, and TN groupings). More studies still need to verify the results for making uniform standards for DCE-MRI in the future. A certain category of radiomics features were also used to evaluate their predictive ability for chemotherapy response, such as Riesz wavelets,⁴⁷ entropy,⁴¹ and the histogram features.⁴⁴ In addition, previous work was focused on intratumoral region to analyze the tumor's physiological environment, however, peritumoral region surrounded the tumor lesion has also been found to be associated with outcomes. Braman *et al*³⁷ combined intratumoral and peritumoral radiomics feature for the evaluation of pCR, yielding a maximum AUC of 0.74 within the testing set. Combining intratumoral and peritumoral radiomics analysis seemed to be a more successful approach to predict NAC. All above studies were concentrated on radiomics features, the clinical information added to the radiomics features seemed to achieve a better performance for prediction. Liu *et al*⁴² built a model named radiomics of multi-parametric magnetic resonance imaging (RMM) combining both multi-parametric MRI and clinical information to predict pCR to NAC in patients with breast cancer. The RMM models improved prognostic accuracy than clinical models and radiomics signatures in the primary cohort and other 3 external validation cohort.⁴² Quantitative analyses extracted from MRI provide a promising tool for predicting tumor response of patients with advanced breast cancer and show the potential and practical value in the clinic.

Prediction of Survival Outcomes in Patients With Breast Cancer

Survival outcome is one of the great concerns for patients with breast cancer. In previous studies, the characteristics of tumors, such as histological tumor grade, LN status, stage, and some biomarkers are common factors to evaluate the patients' prognosis. Recently, some studies evaluated the association between survival outcomes of patients with breast cancer and texture features extracted from imaging (Table 5).⁴⁸⁻⁵² Imaging features could reflect the whole tumor's heterogeneity that may interpret differently with survival outcomes of patients having breast cancer with the same stage. For example, tumor with higher entropy and lower uniformity extracted from T2WI and with lower entropy and higher uniformity extracted from contrast-enhanced T1WI had poorer outcomes.⁴⁸ Park *et al*⁵¹ found radiomics nomogram combining Rad-score and MRI and clinicopathological findings estimated disease-free survival better than clinicopathological models in patients with invasive breast cancer. Three GLCM-related features which had different mathematical definitions were selected. They measured various aspects of tumor texture heterogeneity. Previous studies have evaluated the association between imaging features and pCR, however, pCR is not an accurate surrogate end point for survival. Especially for those patients having early breast cancer with breast-conserving

surgery, whether chemotherapy could bring patients more benefits for survival than adverse side effects. Chan *et al*⁴⁹ evaluated a radiomics model to distinguish between patients at high risk and low risk with a long-term follow-up based on eigentumor analysis. The eigentumors had potentials to stratify patient survival after 140 months with a hazard ratio of 4.31.⁴⁹ Radiomics features for assessing tumor heterogeneity could be regarded as a useful noninvasive biomarker to predict survival of patients with breast cancer and can provide a great benefit for clinical management.

Outlook and Challenges

Magnetic resonance imaging has been extensively used in the diagnosis of breast cancer, predicting malignancy of tumors, staging, evaluating the response to chemotherapy, biopsy guidance, and so on. As the high-throughput data extracted from imaging have conducted a number of "omics" researches. Radiomics of MRI imaging can provide large potential data to characterize the biological features of tumors for precision medicine. Therefore, the utilization of radiomics is hopeful to be an imaging biomarker and noninvasive tool for early diagnosis and evaluation of therapeutic effect in breast cancer. In recent years, genomics, transcriptomics, proteomics, and metabolomics are used to characterize molecular biology of tumors, which were helpful for personalized therapy.^{102,103} Although lots of published studies have evaluated the application for years, the association between other omics technologies and radiomics in breast cancer is not very clear and need to be explored in further researches. Integrations of multi-omics studies can greatly increase the accuracy of diagnosis and provide individualized treatment for patients to prolong the survival time and improve the quality of life. Moreover, other new emerging MRI technologies, such as sodium imaging,¹⁰⁴ chemical exchange saturation transfer imaging,¹⁰⁵ blood oxygen level-dependent,¹⁰⁶ or arterial spin labeling MRI¹⁰⁷ are hopeful to provide high-quality imaging for feature extraction.

Radiomics has been applied in scientific research but not widely in the clinic. Some obstacles have existed and need to be improved by the perfection of technologies and methodology. First, the sample size of radiomics analyses plays an important role in predictive models, as the larger samples can increase prognostic accuracy. However, the samples of most published studies are not very large and the models should be validated in further research. Second, because of imaging acquisition from different machines, varied technical parameters and slice thickness, as well as diverse reconstruction algorithms, it is difficult to acquire consistent imaging and get uniform results that can be applied in the clinic. Third, image segmentation includes automatic, semiautomatic, and manual methods. Automatic and semiautomatic segmentation is more convenient for large data, however, the algorithms of segmentation remain to be evaluated.¹⁰⁸ Manual method is time-consuming and the results may be different because of inter- or intrareaders variability.¹⁰⁸

In conclusion, we investigated the workflow and clinical application of radiomics, as well as the outlook and challenges based on published studies. Radiomics has the potential ability of prediction in diagnosis between malignant and benign breast lesions, ALN status, molecular subtypes of breast cancer, tumor response to chemotherapy, and survival outcomes. Radiomics has been widely used in tumor diagnosis and prognosis, however, it is still in the research phase and many efforts should be taken for clinical translation. We also have discussed the limitations and promises of radiomics for improvement in further research. Our study aims are to help clinicians and radiologists to get to know the basic information of radiomics and encourage cooperation with scientists to mine data for a better application in clinical practice.

Authors' Note

Our study did not require an ethical board approval because it did not contain human or animal trials.


Declaration of Conflicting Interests

The author(s) declared no potential conflicts of interest with respect to the research, authorship, and/or publication of this article.

Funding

The author(s) received no financial support for the research, authorship, and/or publication of this article.

ORCID iD

Dong-Man Ye  <https://orcid.org/0000-0002-2901-0283>

References

- Bray F, Ferlay J, Soerjomataram I, Siegel RL, Torre LA, Jemal A. Global cancer statistics 2018: GLOBOCAN estimates of incidence and mortality worldwide for 36 cancers in 185 countries. *CA Cancer J Clin.* 2018;68(6):394-424.
- Allemani C, Weir HK, Carreira H, et al. Global surveillance of cancer survival 1995-2009: analysis of individual data for 25,676,887 patients from 279 population-based registries in 67 countries (CONCORD-2). *Lancet.* 2015;385(9972):977-1010.
- Lambin P, Rios-Velazquez E, Leijenaar R, et al. Radiomics: extracting more information from medical images using advanced feature analysis. *Eur J Cancer.* 2012;48(4):441-446.
- Kumar V, Gu Y, Basu S, et al. Radiomics: the process and the challenges. *Magn Reson Imaging.* 2012;30(9):1234-1248.
- Gillies RJ, Kinahan PE, Hricak H. Radiomics: images are more than pictures, they are data. *Radiology.* 2016;278(1):563-577.
- Bahreini L, Fatemizadeh E, Guity M. Physics Diagnostic efficacy of all series of dynamic contrast enhanced breast MR images using gradient vector flow (GVF) segmentation and novel border feature extraction for differentiation between malignant and benign breast lesions. *Iran J Radiol.* 2010;7:225-234.
- Bickelhaupt S, Jaeger PF, Laun FB, et al. Radiomics based on adapted diffusion kurtosis imaging helps to clarify most mammographic findings suspicious for cancer. *Radiology.* 2018;287(3):761-770.
- Bickelhaupt S, Paech D, Kickingeder P, et al. Prediction of malignancy by a radiomic signature from contrast agent-free diffusion MRI in suspicious breast lesions found on screening mammography. *J Magn Reson Imaging.* 2017;46(2):604-616.
- Holli K, Lääperi AL, Harrison L, et al. Characterization of breast cancer types by texture analysis of magnetic resonance images. *Acad Radiol.* 2010;17(2):135-141.
- Hu B, Xu K, Zhang Z, Chai R, Li S, Zhang L. A radiomic nomogram based on an apparent diffusion coefficient map for differential diagnosis of suspicious breast findings. *Chin J Cancer Res.* 2018;30(4):432-438.
- Jiang X, Xie F, Liu L, Peng Y, Cai H, Li L. Discrimination of malignant and benign breast masses using automatic segmentation and features extracted from dynamic contrast-enhanced and diffusion-weighted MRI. *Oncol Lett.* 2018;16(2):1521-1528.
- Karahaliou A, Vassiou K, Arikidis NS, Skiadopoulou S, Kanavou T, Costaridou L. Assessing heterogeneity of lesion enhancement kinetics in dynamic contrast-enhanced MRI for breast cancer diagnosis. *Br J Radiol.* 2010;83(988):296-309.
- Nie K, Chen JH, Yu HJ, Chu Y, Nalcioglu O, Su MY. Quantitative analysis of lesion morphology and texture features for diagnostic prediction in breast MRI. *Acad Radiol.* 2008;15(12):1513-1525.
- Whitney HM, Drukker K, Edwards A, et al. Effect of biopsy on the MRI radiomics classification of benign lesions and luminal A cancers. *J Med Imaging.* 2019;6(3):031408.
- Gibbs P, Turnbull LW. Textural analysis of contrast-enhanced MR images of the breast. *Magn Reson Med.* 2003;50(1):92-98.
- Chai R, Ma H, Xu M, et al. Differentiating axillary lymph node metastasis in invasive breast cancer patients: a comparison of radiomic signatures from multiparametric breast MR sequences. *J Magn Reson Imaging.* 2019;50(4):1125-1132.
- Cui X, Wang N, Zhao Y, et al. Preoperative prediction of axillary lymph node metastasis in breast cancer using radiomics features of DCE-MRI. *Sci Rep.* 2019;9(1):2240.
- Dong Y, Feng Q, Yang W, et al. Preoperative prediction of sentinel lymph node metastasis in breast cancer based on radiomics of T2-weighted fat-suppression and diffusion-weighted MRI. *Eur Radiol.* 2018;28(2):582-591.
- Han L, Zhu Y, Liu Z, et al. Radiomic nomogram for prediction of axillary lymph node metastasis in breast cancer. *Eur Radiol.* 2019;29(7):3820-3829.
- Liu C, Ding J, Spuhler K, et al. Preoperative prediction of sentinel lymph node metastasis in breast cancer by radiomic signatures from dynamic contrast-enhanced MRI. *J Magn Reson Imaging.* 2019;49(1):131-140.
- Liu Z, Feng B, Li C, et al. Preoperative prediction of lymphovascular invasion in invasive breast cancer with dynamic contrast-enhanced-MRI-based radiomics. *J Magn Reson Imaging.* 2019;50(3):847-857.
- Holli-Helenius K, Salminen A, Rinta-Kiikka I, et al. MRI texture analysis in differentiating luminal A and luminal B breast cancer molecular subtypes - a feasibility study. *BMC Med Imag.* 2017;17(2):69.
- Fan M, Cheng H, Zhang P, et al. DCE-MRI texture analysis with tumor subregion partitioning for predicting Ki-67 status of

- estrogen receptor-positive breast cancers. *J Magn Reson Imaging*. 2018;48(1):237-247.
24. Fan M, Li H, Wang S, Zheng B, Zhang J, Li L. Radiomic analysis reveals DCE-MRI features for prediction of molecular subtypes of breast cancer. *PLoS One*. 2017;12(2):e0171683.
 25. Fan M, Zhang P, Wang Y, et al. Radiomic analysis of imaging heterogeneity in tumours and the surrounding parenchyma based on unsupervised decomposition of DCE-MRI for predicting molecular subtypes of breast cancer. *Eur Radiol*. 2019;29(8):4456-4467.
 26. Grimm LJ, Zhang J, Mazurowski MA. Computational approach to radiogenomics of breast cancer: luminal A and luminal B molecular subtypes are associated with imaging features on routine breast MRI extracted using computer vision algorithms. *J Magn Reson Imaging*. 2015;42(4):902-907.
 27. Juan M-W, Yu J, Peng GX, Jun LJ, Feng SP, Fang LP. Correlation between DCE-MRI radiomics features and Ki-67 expression in invasive breast cancer. *Oncol Lett*. 2018;16(4):5084-5090.
 28. Ko ES, Kim JH, Lim Y, Han BK, Cho EY, Nam SJ. Assessment of invasive breast cancer heterogeneity using whole-tumor magnetic resonance imaging texture analysis: correlations with detailed pathological findings. *Medicine (Baltimore)*. 2016;95(3):e2453.
 29. Liang C, Cheng Z, Huang Y, et al. An MRI-based radiomics classifier for preoperative prediction of Ki-67 status in breast cancer. *Acad Radiol*. 2018;25(9):1111-1117.
 30. Ma W, Ji Y, Qi L, Guo X, Jian X, Liu P. Breast cancer Ki67 expression prediction by DCE-MRI radiomics features. *Clin Radiol*. 2018;73(10):909. e1-909.e5.
 31. Monti S, Aiello M, Incoronato M, et al. DCE-MRI pharmacokinetic-based phenotyping of invasive ductal carcinoma: A radiomic study for prediction of histological outcomes. *Contrast Media Mol Imaging*. 2018;2018:5076269.
 32. Saha A, Harowicz MR, Grimm LJ, et al. A machine learning approach to radiogenomics of breast cancer: a study of 922 subjects and 529 DCE-MRI features. *Br J Cancer*. 2018;119(4):508-516.
 33. Sun X, He B, Luo X, et al. Preliminary study on molecular subtypes of breast cancer based on magnetic resonance imaging texture analysis. *J Comput Assist Tomogr*. 2018;42(4):531-535.
 34. Wang J, Kato F, Oyama-Manabe N, et al. Identifying triple-negative breast cancer using background parenchymal enhancement heterogeneity on dynamic contrast-enhanced MRI: a pilot radiomics study. *PLoS One*. 2015;10(11):e0143308.
 35. Xie T, Zhao Q, Fu C, et al. Differentiation of triple-negative breast cancer from other subtypes through whole-tumor histogram analysis on multiparametric MR imaging. *Eur Radiol*. 2019;29(5):2535-2544.
 36. Ahmed A, Gibbs P, Pickles M, Turnbull L. Texture analysis in assessment and prediction of chemotherapy response in breast cancer. *J Magn Reson Imaging*. 2013;38(1):89-101.
 37. Braman NM, Etesami M, Prasanna P, et al. Intratumoral and peritumoral radiomics for the pretreatment prediction of pathological complete response to neoadjuvant chemotherapy based on breast DCE-MRI. *Breast Cancer Res*. 2017;19(1):57.
 38. Cain EH, Saha A, Harowicz MR, Marks JR, Marcom PK, Mazurowski MA. Multivariate machine learning models for prediction of pathologic response to neoadjuvant therapy in breast cancer using MRI features: a study using an independent validation set. *Breast Cancer Res Treat*. 2019;173(2):455-463.
 39. Chamming's F, Ueno Y, Ferre R, et al. Features from computerized texture analysis of breast cancers at pretreatment MR imaging are associated with response to neoadjuvant chemotherapy. *Radiology*. 2018;286(1):412-420.
 40. Fan M, Wu G, Cheng H, Zhang J, Shao G, Li L. Radiomic analysis of DCE-MRI for prediction of response to neoadjuvant chemotherapy in breast cancer patients. *Eur J Radiol*. 2017;94:140-147.
 41. Henderson S, Purdie C, Michie C, et al. Interim heterogeneity changes measured using entropy texture features on T2-weighted MRI at 3.0 T are associated with pathological response to neoadjuvant chemotherapy in primary breast cancer. *Eur Radiol*. 2017;27(11):4602-4611.
 42. Liu Z, Li Z, Qu J, et al. Radiomics of multi-parametric MRI for pretreatment prediction of pathological complete response to neoadjuvant chemotherapy in breast cancer: a multicenter study. *Clin Cancer Res*. 2019;25(12):3538-3547.
 43. Michoux N, Van den Broeck S, Lacoste L, et al. Texture analysis on MR images helps predicting non-response to NAC in breast cancer. *BMC cancer*. 2015;15.
 44. Panzeri MM, Losio C, Della Corte A, et al. Prediction of chemoresistance in women undergoing neo-adjuvant chemotherapy for locally advanced breast cancer: volumetric analysis of first-order textural features extracted from multiparametric MRI. *Contrast Media Mol Imaging*. 2018;2018:8329041.
 45. Teruel JR, Heldahl MG, Goa PE, et al. Dynamic contrast-enhanced MRI texture analysis for pretreatment prediction of clinical and pathological response to neoadjuvant chemotherapy in patients with locally advanced breast cancer. *NMR Biomed*. 2014;27(8):887-896.
 46. Wu J, Gong G, Cui Y, Li R. Intratumor partitioning and texture analysis of dynamic contrast-enhanced (DCE)-MRI identifies relevant tumor subregions to predict pathological response of breast cancer to neoadjuvant chemotherapy. *J Magn Reson Imaging*. 2016;44(5):1107-1115.
 47. Banerjee I, Malladi S, Lee D, et al. Assessing treatment response in triple-negative breast cancer from quantitative image analysis in perfusion magnetic resonance imaging. *J Med Imaging (Bellingham)*. 2018;5(1):011008.
 48. Kim JH, Ko ES, Lim Y, et al. Breast cancer heterogeneity: MR imaging texture analysis and survival outcomes. *Radiology*. 2017;282(3):665-675.
 49. Chan HM, van der Velden BHM, Loo CE, Gilhuijs KGA. Eigentumors for prediction of treatment failure in patients with early-stage breast cancer using dynamic contrast-enhanced MRI: a feasibility study. *Phys Med Biol*. 2017;62(16):6467-6485.
 50. Drukker K, Li H, Antropova N, Edwards A, Papaioannou J, Giger ML. Most-enhancing tumor volume by MRI radiomics predicts recurrence-free survival "early on" in neoadjuvant treatment of breast cancer. *Cancer Imaging*. 2018;18(1):12.

51. Park H, Lim Y, Ko ES, et al. Radiomics signature on magnetic resonance imaging: Association with disease-free survival in patients with invasive breast cancer. *Clin Cancer Res.* 2018; 24(19):4705-4714.
52. Pickles MD, Lowry M, Gibbs P. Pretreatment prognostic value of dynamic contrast-enhanced magnetic resonance imaging vascular, texture, shape, and size parameters compared with traditional survival indicators obtained from locally advanced breast cancer patients. *Invest Radiol.* 2016;51(3):177-185.
53. Mao L, Chen H, Liang M, et al. Quantitative radiomic model for predicting malignancy of small solid pulmonary nodules detected by low-dose CT screening. *Quant Imaging Med Surg.* 2019;9(2): 263-272.
54. He L, Huang Y, Ma Z, Liang C, Liang C, Liu Z. Effects of contrast-enhancement, reconstruction slice thickness and convolution kernel on the diagnostic performance of radiomics signature in solitary pulmonary nodule. *Sci Rep.* 2016;6:34921.
55. Chen B, Zhang R, Gan Y, et al. Development and clinical application of radiomics in lung cancer. *Radiat Oncol.* 2017;12(1): 154-154.
56. Limkin EJ, Sun R, Dercle L, et al. Promises and challenges for the implementation of computational medical imaging (radiomics) in oncology. *Ann Oncol.* 2017;28(6):1191-1206.
57. Lee G, Lee HY, Park H, et al. Radiomics and its emerging role in lung cancer research, imaging biomarkers and clinical management: state of the art. *Eur J Radiol.* 2017;86(5):297-307.
58. Haralick RM, Shanmugam K. Textural features for image classification. *IEEE Transact Syst, Man, Cybernet.* 1973;610-621.
59. Galloway MM. Texture analysis using grey level run lengths. *NASA STI/Recon Technical Report N.* 1974;75.
60. Thibault G, Angulo J, Meyer F. Advanced statistical matrices for texture characterization: application to cell classification. *IEEE Transactions on Biomedical Enginee.* 2014;61(3):630-637.
61. Sun C, Wee WG. Neighboring gray level dependence matrix for texture classification. *Comput Vision, Graph Image Process.* 1983;23(4):341-352.
62. Parmar C, Grossmann P, Bussink J, et al. Machine learning methods for quantitative radiomic biomarkers. *Sci Rep.* 2015;5:13087.
63. Prasanna P, Tiwari P, Madabhushi A. Co-occurrence of local anisotropic gradient orientations (CoLIAGe): a new radiomics descriptor. *Sci Rep.* 2016;6(1):37241.
64. Bickelhaupt S, Laun FB, Tesdorff J, et al. Fast and noninvasive characterization of suspicious lesions detected at breast cancer X-ray screening: capability of diffusion-weighted MR Imaging with MIPs. *Radiology.* 2016;278(4):689-697.
65. Pinker K, Helbich TH, Morris EA. The potential of multiparametric MRI of the breast. *Br J Radiol.* 2017;90(1069):20160715.
66. Partridge SC, Nissan N, Rahbar H, Kitsch AE, Sigmund EE. Diffusion-weighted breast MRI: clinical applications and emerging techniques. *J Magn Reson Imaging.* 2017;45(2):337-355.
67. Zhang L, Tang M, Min Z, et al. Accuracy of combined dynamic contrast-enhanced magnetic resonance imaging and diffusion-weighted imaging for breast cancer detection: a meta-analysis. *Acta Radiol.* 2016;57(1):651-660.
68. Li XR, Cheng LQ, Liu M, et al. DW-MRI ADC values can predict treatment response in patients with locally advanced breast cancer undergoing neoadjuvant chemotherapy. *Med Oncol.* 2012;29(2): 425-431.
69. Sharma U, Danishad KKA, Seenu V, Jagannathan NR. Longitudinal study of the assessment by MRI and diffusion-weighted imaging of tumor response in patients with locally advanced breast cancer undergoing neoadjuvant chemotherapy. *NMR Biomed.* 2009;22(1):104-113.
70. Le Bihan D, Mangin JF, Poupon C, et al. Diffusion tensor imaging: concepts and applications. *J Magn Reson Imaging.* 2001; 13(4):534-546.
71. Partridge SC, Ziadloo A, Murthy R, et al. Diffusion tensor MRI: preliminary anisotropy measures and mapping of breast tumors. *J Magn Reson Imaging.* 2010;31(2):339-347.
72. Le Bihan D. What can we see with IVIM MRI? *Neuroimage.* 2019;187(5):56-67.
73. Iima M, Honda M, Sigmund EE, et al. Diffusion MRI of the breast: current status and future directions. *J Magn Reson Imaging.* 2019. doi:10.1002/jmri.26908.
74. Li H, Sun H, Liu S, et al. Assessing the performance of benign and malignant breast lesion classification with bilateral TIC differentiation and other effective features in DCE-MRI. *J Magn Reson Imaging.* 2019;50(2):465-473.
75. Fischer U, Kopka L, Grabbe E. Breast carcinoma: effect of preoperative contrast-enhanced MR imaging on the therapeutic approach. *Radiology.* 1999;213(2):881-888.
76. Warren RM, Pointon L, Thompson D, et al. Reading protocol for dynamic contrast-enhanced MR images of the breast: sensitivity and specificity analysis. *Radiology.* 2005;236:779-788.
77. Turnbull LW. Dynamic contrast-enhanced MRI in the diagnosis and management of breast cancer. *NMR Biomed.* 2009;22:28-39.
78. Gonzalez-Huebra I, Elizalde A, Garcia-Baizan A, et al. Is it worth to perform preoperative MRI for breast cancer after mammography, tomosynthesis and ultrasound? *Magnet Reson Imag.* 2019; 57:317-322.
79. DeMartini WB, Liu F, Peacock S, Eby PR, Gutierrez RL, Lehman CD. Background parenchymal enhancement on breast MRI: impact on diagnostic performance. *AJR Am J Roentgenol.* 2012; 198(4):W373-W380.
80. Hambly NM, Liberman L, Dershaw DD, Brennan S, Morris EA. Background parenchymal enhancement on baseline screening breast MRI: impact on biopsy rate and short-interval follow-up. *AJR Am J Roentgenol.* 2011;196(1):218-224.
81. Losurdo L, Basile TMA, Fanizzi A, et al. A gradient-based approach for breast DCE-MRI analysis. *Biomed Res Int.* 2018; 2018:9032408.
82. O'Grady S, Morgan MP. Microcalcifications in breast cancer: from pathophysiology to diagnosis and prognosis. *Biochim Biophys Acta Rev Cancer.* 2018;1869(2):310-320.
83. Losurdo AFL, Basile TMA. *A Combined Approach of Multiscale Texture Analysis and Interest Point/Corner Detectors for Microcalcifications Diagnosis.* Springer, Cham: IWBBIO; 2018.
84. Giuliano AE, Ballman KV, McCall L, et al. Effect of axillary dissection vs no axillary dissection on 10-year overall survival among women with invasive breast cancer and sentinel node metastasis: the ACOSOG Z0011 (Alliance) randomized clinical trial. *JAMA.* 2017;318(10):918-926.

85. Lyman GH, Somerfield MR, Bosserman LD, Perkins CL, Weaver DL, Giuliano AE. Sentinel lymph node biopsy for patients with early-stage breast cancer: American society of clinical oncology clinical practice guideline update. *J Clin Oncol*. 2017;35(5):561-564.
86. Giuliano AE, Hunt KK, Ballman KV, et al. Axillary dissection vs no axillary dissection in women with invasive breast cancer and sentinel node metastasis: a randomized clinical trial. *JAMA*. 2011;305(6):569-575.
87. Perou CM, Sorlie T, Eisen MB, et al. Molecular portraits of human breast tumours. *Nature*. 2000;406(6797):747-752.
88. Blows FM, Driver KE, Schmidt MK, et al. Subtyping of breast cancer by immunohistochemistry to investigate a relationship between subtype and short and long term survival: a collaborative analysis of data for 10,159 cases from 12 studies. *PLoS Med*. 2010;7(5):e1000279.
89. Perou CM, Borresen-Dale AL. Systems biology and genomics of breast cancer. *Cold Spring Harb Perspect Biol*. 2011;3(2):a003293.
90. Carey LA, Dees EC, Sawyer L, et al. The triple negative paradox: primary tumor chemosensitivity of breast cancer subtypes. *Clin Cancer Res*. 2007;13(8):2329-2334.
91. Dilorenzo G, Telegrafo M, La Forgia D, Stabile Ianora AA, Moschetta M. Breast MRI background parenchymal enhancement as an imaging bridge to molecular cancer sub-type. *Eur J Radiol*. 2019;113:148-152.
92. Montemezzi S, Camera L, Giri MG, et al. Is there a correlation between 3 T multiparametric MRI and molecular subtypes of breast cancer? *Eur J Radiol*. 2018;108:120-127.
93. Esteva FJ, Hortobagyi GN. Prognostic molecular markers in early breast cancer. *Breast Cancer Res*. 2004;6(3):109-118.
94. King AD, Chow KK, Yu KH, et al. Head and neck squamous cell carcinoma: diagnostic performance of diffusion-weighted MR imaging for the prediction of treatment response. *Radiology*. 2013;266(2):531-538.
95. Foroutan P, Krehling JM, Morse DL, et al. Diffusion MRI and novel texture analysis in osteosarcoma xenotransplants predicts response to anti-checkpoint therapy. *PLoS One*. 2013;8(12):e82875.
96. Ambikapathi A, Chan TH, Lin CH, Yang FS, Chi CY, Wang Y. Convex-optimization-based compartmental pharmacokinetic analysis for prostate tumor characterization using DCE-MRI. *IEEE Trans Biomed Eng*. 2016;63(4):707-720.
97. Chen L, Choyke PL, Wang N, et al. Unsupervised deconvolution of dynamic imaging reveals intratumor vascular heterogeneity and repopulation dynamics. *PLoS One*. 2014;9(11):e112143.
98. Mauri D, Pavlidis N, Ioannidis JP. Neoadjuvant versus adjuvant systemic treatment in breast cancer: a meta-analysis. *J Natl Cancer Inst*. 2005;97(3):188-194.
99. Rouzier R, Perou CM, Symmans WF, et al. Breast cancer molecular subtypes respond differently to preoperative chemotherapy. *Clin Cancer Res*. 2005;11(16):5678-5685.
100. Cortazar P, Zhang L, Untch M, et al. Pathological complete response and long-term clinical benefit in breast cancer: the CTNeoBC pooled analysis. *Lancet*. 2014;384(9938):164-172.
101. Eisenhauer EA, Therasse P, Bogaerts J, et al. New response evaluation criteria in solid tumours: revised RECIST guideline (version 1.1). *Eur J Cancer*. 2009;45(2):228-247.
102. Aerts HJ, Velazquez ER, Leijenaar RT, et al. Decoding tumour phenotype by noninvasive imaging using a quantitative radiomics approach. *Nat Commun*. 2014;5:4006.
103. Pinker K, Chin J, Melsaether AN, Morris EA, Moy L. Precision medicine and radiogenomics in breast cancer: new approaches toward diagnosis and treatment. *Radiology*. 2018;287(3):732-747.
104. Zaric O, Pinker K, Zbyn S, et al. Quantitative sodium MR imaging at 7 T: initial results and comparison with diffusion-weighted imaging in patients with breast tumors. *Radiology*. 2016;280(1):39-48.
105. Jones KM, Pollard AC, Pagel MD. Clinical applications of chemical exchange saturation transfer (CEST) MRI. *J Magn Reson Imaging*. 2018;47(1):11-27.
106. King AD, Thoeny HC. Functional MRI for the prediction of treatment response in head and neck squamous cell carcinoma: potential and limitations. *Cancer Imaging*. 2016;16(1):23.
107. Nudelman KN, Wang Y, McDonald BC, et al. Altered cerebral blood flow one month after systemic chemotherapy for breast cancer: a prospective study using pulsed arterial spin labeling MRI perfusion. *PLoS One*. 2014;9(5):e96713.
108. Sala E, Mema E, Himoto Y, et al. Unravelling tumour heterogeneity using next-generation imaging: radiomics, radiogenomics, and habitat imaging. *Clin Radiol*. 2017;72(1):3-10.